Microstructural evaluation of Al-2.5wt.%Mg-0.7wt.%Li in as cast condition

Kozina, Franjo; Zovko Brodarac, Zdenka; Petrič, Mitja

16th INTERNATIONAL FOUNDRYMEN CONFERENCE
Global Foundry Industry – Perspectives for the Future
Opatija, May 15th-17th, 2017

MICROSTRUCTURAL EVALUATION OF Al - 2.5wt.%Mg – 0.7wt.%Li ALLOY IN AS CAST CONDITION

Franjo Kozina[1], Zdenka Zovko Brodarac[1], Mitja Petrič[2]

[1]University of Zagreb Faculty of Metallurgy, Sisak, Croatia
[2]University of Ljubljana Faculty of Natural Sciences and Engineering, Ljubljana, Slovenia

Oral presentation
Original scientific paper

Abstract

The intention of designing of innovative engineering materials with advanced properties found its role in special purposes, such as aerospace application. The main issue has been recognized as a weight savings, stiffness development and mechanical properties. Lithium, in Al-Mg-Li alloys, plays a significant role through stimulation of precipitation hardening, increasing of Young's modulus, stiffness, fracture toughness and enhancing corrosion resistance. Other significant alloying element such as magnesium influences strengthening effect by enhancing the precipitation of metastable δ' (Al_3Li) phase. This indirect strengthening effect is possible due to fact that magnesium reduces solubility of lithium in aluminium. While the mechanism of this indirect strengthening seems to be simple, it is not fully understood if presence of magnesium merely changes the phase stability, interfacial energy or diffusion coefficient. In order to understand magnesium role in Al-Mg-Li ternary system, Al-2.5wt.%Mg–0.7wt.%Li was produced under laboratory conditions. Obtained results of Thermo-Calc calculations and microstructural investigation enabled valuation of solidification sequence and micro constituent's development and/or transformation.

***Keywords**: Al-Mg-Li alloy, lithium, magnesium, density, phase precipitation*

*Corresponding author (e-mail address): *fkozin@simet.hr*

INTRODUCTION

The interest in the aluminium-lithium alloys is fuelled by three important considerations: reduction of density, increase in elastic modulus and introduction of precipitation hardening by the formation of metastable δ' (Al_3Li) phase [1]. Because the unique combination of properties provided by aluminium (Al) and Al based alloys [2], it is not surprising that they have been utilized in the aircraft construction since 1930., manly those of 2XXX and 7XXX series [3]. However, despite their low specific density, wide interval of strength properties,

good workability, corrosion resistance and electrical and thermal conductivity, stiffness represents a problem when using Al and Al based alloys, due to their low Young's modulus [4]. Onwards, the need for further weight reduction and higher stiffness indicated a need for chemical composition redesign [5]. The key alloying elements contributing to the reduction in density of Al based alloys are lithium (Li), calcium (Ca), magnesium (Mg) and beryllium (Be) [6]. But from the aforementioned elements, Li has been found the most effective addition to reduce density of commercial Al alloys as well as to stimulate the precipitation hardening, increase stiffness, fracture toughness and enhance corrosion resistance [7]. Besides Be, associated with health and manufacturing problems, Li is the only metal that significantly improves elastic modulus, as illustrated in Figure 1 [8]. Namely, every 1% of Li added to Al alloys increases elastic modulus roughly for 3 GPa and decreases density by approximately 80 kg/m^3 [9] for the addition up to 4% [10]. As a consequence Al-Li based alloys have high specific modulus and specific strength, allowing large weight savings in aircraft structures. Just to illustrate, direct substitution of traditional Al based alloys for Al-Li alloys can yield to ~11% weight savings, while complete redesign of aircraft utilizing their full potential up to ~17% of weight savings [11]. Furthermore, Li has a high solubility in Al reaching up to 14% at 600°C which respectively decreases with temperature decrease, consequently opening the possibility for modelling mechanical properties by artificial aging [12].

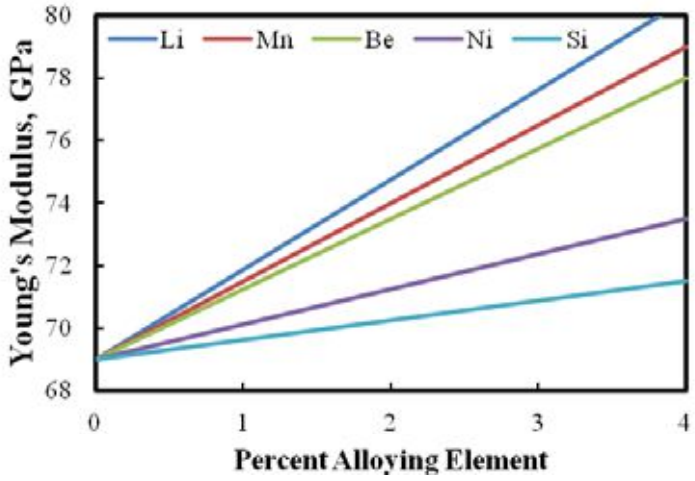

Figure 1. Impact of alloying elements on Young's modulus of Al based alloys [13]

Consequently, a several microstructural features are found to be unique for these alloys: nature and volume fraction of strengthening precipitates, amount of co-precipitates that alter the planar slip deformation behaviour, width of the precipitate free zone (PFZ) and the content, size and distribution of coarse and angular equilibrium precipitates [14]. The nature, structure, size and distribution of the precipitates are influenced by chemical composition and heat treatment parameters [15]. This microstructural features have pronounced effect on the mechanical behaviour of these alloys [16]. While the PFZ contribute to the formation of cracks at the grain boundaries leading to the fatigue and corrosion resistance decrease [17], the precipitates can interact with dislocations therefore significantly increasing anisotropy originating from microstructural texture [18], as well as increase of sensitivity to long term low temperature exposure [19]. Onwards, insoluble

constituents of second-phase particles (often aided by trace elements, such as sodium (Na) and potassium (K) lead to low ductility and fracture toughness [20].

Alloying additions of copper (Cu), zirconium (Zr), silver (Ag) or Mg, minimize those problems by interdicting new precipitates and changing the nucleation characteristic of existing metastable δ' phase [16]. Besides solid solution and precipitation strengthening, Mg leads to further density reductions as well.

Based on this, several Al-Li-Mg alloys have been developed and utilized. They are represented by grades 1420, 1421 and 1423. Initially, it was established that alloying Al-Mg alloys with Li has a little effect on their mechanical properties and that it does not results with improvements during heat treatment. However, this claim was disputed after development of 1420 alloy in 1965, which was 10-12% lighter than any other Al-Li-X alloys used at that time. The chemical composition and density of commercially used Al-Li-Mg alloy is given in Table 1. Relatively higher concentrations of Li and Mg are required to compensate for the presence of much heavier elements such as zirconium (Zr) and scandium (Sc). Besides, 1420 alloy had a high corrosion resistance, good weldability, high elastic modulus and static tensile strength [21]. On the other hand, Mg additions can cause small decrease in elastic modulus [18].

Table 1. Chemical composition and density of commercially used Al-Li-Mg alloys[1]

Alloy	Li, wt.%	Mg, wt.%	Zr, wt.%	Sc, wt.%	Al, wt.%	ρ, g/cm^3
1420	2.1	5.2	0.11	-	Bal.	2.47
1421	2.1	5.2	0.11	0.17	Bal.	2.47
1423	1.9	3.5	-	-	Bal.	-

Although, precipitation in Al-Li-Mg and Al-Li system seem to be similar, it is suspected that Mg decreases solubility of Li in α_{Al} matrix enhancing the precipitation of metastable δ' phase [22]. During that time, parameters of α_{Al} lattice become enhanced due to the Mg enrichment. Onwards, at higher temperatures, metastable δ' phase transforms into ternary phase T (Al_2MgLi) with a complex cubic lattice. Mg from the enriched α_{Al} precipitates to the ternary T phase consequently decreasing its lattice parameters and increasing ductility [23]. Although this system seems quite simple, the precise distribution of Mg atoms between matrix and metastable δ' phase is not fully understood. Onwards, it is not clear if the precipitation enhancement, due to Mg addition, is mainly controlled by the phase stability, changes in interfacial energy or changes in diffusion coefficient [24].

In order to understand mechanism of phase precipitations and Mg distribution in Al-Mg-Li ternary system, Al-2.5wt%Mg–0.7wt%Li was produced under laboratory conditions. Computer aided thermodynamic diagram calculation (CALPHAD) enabled the extrapolation of particular multicomponent alloy and prediction of corresponded solidification sequence. Correlation of obtained results with microstructural analysis reveals identification of present constituents and theirs behaviour.

MATERIALS AND METHODS

Due to high reactivity of Li with molten alloy, crucible materials and open atmosphere,

melting and casting of Al-Li based alloys represents a challenge. To minimize Li reactivity and a following loss, three different melting procedures have been developed: alloying with Al-Li master alloy (containing up to 20 % of Li), melting under a flux cover and Li addition under vacuum or inert atmosphere [6].

The Al block (technical purity), placed into a graphite crucible coated with boron-nitrite has been deposited into induction melting furnace. Controlled atmosphere was maintained by Ar introduction and crucible cover, Figure 2a. The Al block was melted at 720 °C, followed by Mg addition. A steel bell coated with boron-nitrite was used for introduction of Li, wrapped in Al-foil (commercial purity) into a molten alloy, and stirring to ensure a homogeneous distribution of Li in the melt. Casting was performed into a steel mould at 700 °C without protective atmosphere (Figure 2b).

a) b)

Figure 2. Induction furnace and steel mould:
a) Melting process of Al-2.5wt%Mg–0.7wt%Li alloy
b) Steel mold after casting of Al-2.5wt%Mg–0.7wt%Li alloy

In order to establish a loss of Li and Mg during melting and casting, the sample for chemical analysis was taken. The analysis was done using ARL™ 4460 Optical Mass Spectroscope.
In order to calculate density, weight and volume of a whole sample were measured, first. Casting shape and geometry indicates different solidification conditions in corresponding zones. Afterwards, sample was cut into characteristic sections (Figure 3b). The weight and volume of each section were measured as well. Finally, samples for metallographic analysis were taken.

Samples for metallographic analysis were prepared semi-automatically on grinding/polishing machine Pheonix Beta Biller SAD. In order to observe grain size and microstructure, samples were etched. The solution containing 2 parts of hydrofluoric acid, 1 part of nitric acid and 3 parts of glycerine was used to reveal the grain boundaries. Grain boundaries and

microstructure were observed by electrolytic etching using Barker etching solution (5 ml HBF_4 in 200 ml distilled H_2O). Images were taken under polarized light. And finally, Weck's reagent, consisting of 100 ml of water, 4 g of potassium permanganate and 1 g of sodium hydroxide, was used to obtain microstructure. Polarized light was necessary for imaging too.

While Olympus GX51 microscope was used to perform the optical microscopy, electron microscopy was done on Tescan, Vega TS 5136 MM in combination with energy dispersal spectrometer (EDS) Bruker Dispersive Spectrometer.

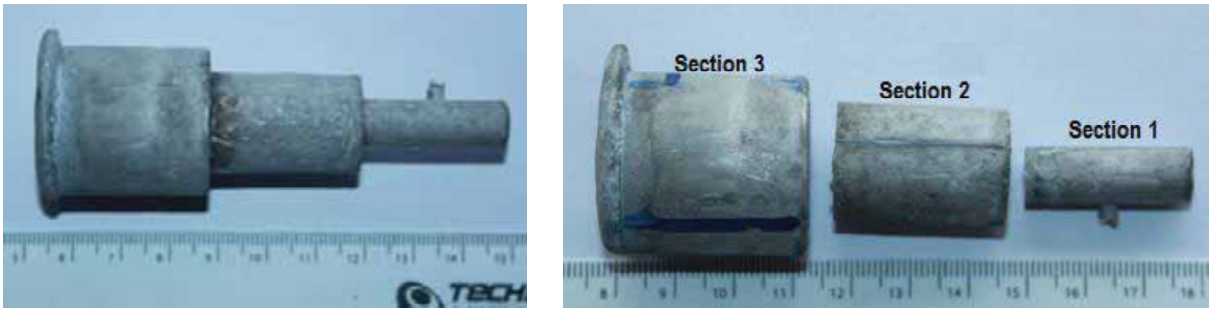

a) b)

Figure 3. The sample of Al-2.wt.Mg-0.7wt.%Li alloy: a) After casting, b) After sampling for density calculations

RESULTS AND DISCUSSION

According to the results of chemical analysis, given in Table 1, 74 wt% of Li added has been lost during melting and casting. Low vapour pressure of Li comprehends its significant loss. Beside this, higher mobility and atomic fraction of Li allows early formation of Li_2O. Although MgO is thermodynamically more stable, Li_2O will start to appear at temperatures slightly above 100°C, much earlier than any other compound in Al-Li-Mg ternary system. Supporting this fact, only 13 wt% of Mg added was lost.

Table 2. Addition of particular element and chemical composition of Al-2.5Mg-0.7Li alloy

Element	Al	Mg	Li
Addition	Bal.	2.8	2.9
wt.%	Bal.	2.480	0.726

Density (ρ) of individual sections and a whole sample is given in Table 3. The lack of deviation in density between individual sections means that all absorbed Li is equally distributed among them. Since the last section is closest to the open atmosphere, and has a lowest cooling rate, somewhat higher density is not surprising.

Table 3. Density value of sample and individual sections

Section	m, g	V, cm^3	ρ, g/cm^3
1	5.432	2.200	2.469
2	22.074	9.0	2.453
3	56.301	22.0	2.559
Sample	84.623	34.0	2.489

Compared to the other commercially used Al based alloys, especially those of 2XXX (2.78 g/cm^3) and 7XXX (2.81-2.86 g/cm^3) series, Al-2.5wt%Mg–0.7wt%Li alloy has a lower density. It can even parry to other commercially used Al-Li-Mg alloys with much higher Li and Mg content (Table 1).

Based on achieved chemical composition, computer aided thermodynamic diagram calculation (CALPHAD) was used to obtain solidification sequence and to see precipitation of stabile phases.

Equilibrium phase diagram obtained by Thermo-Calc software support reveals phase transformation and precipitation, as shown in Figure 4

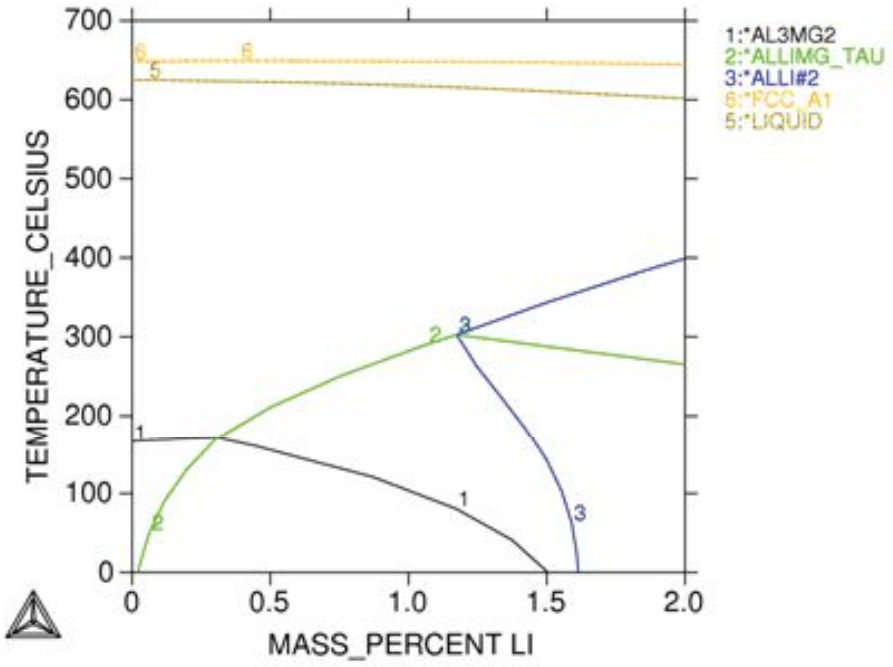

Figure 4. The Al-rich corner of Al-Mg-Li diagram in respect to Li

Solidification sequence according to the equilibrium phase diagram is given in Table 4.

Table 4. Solidification sequence according to Thermo-Calc calculations

Reaction	Temperature, °C
$L \rightarrow \alpha_{Al}$	622
$L + \alpha_{Al} \rightarrow \alpha_{Al}' + AlLi$	368
$\alpha_{Al}' + AlLi \rightarrow \alpha_{Al}'' + Al_2LiMg$	257
$\alpha_{Al}'' \rightarrow \alpha_{Al}''' + Al_3Mg_2$	138

According to the diagram in Figure 4, the equilibrium solidification involves formation of primary Al dendrite development at 622°C, followed by stabile δ (AlLi) phase precipitation. In real solidification conditions for high Li/Mg ratio, metastable δ' phase becomes stabile as δ. In chase that the Li/Mg ratio is low, metastable δ' phase transforms into T phase [1]. In non-equilibrium condition, Mg reduces the solubility of Li in α_{Al}, encouraging metastable δ' phase to develop first. Precipitation of the δ' causes the extraction of Al from the solid solution

leading to the increase in the lattice parameters of α_{Al}. Consequently, Mg content in solid solution increases [23].

The incoherent equilibrium T phase has a complex cubic lattice (a=2.02 nm) [24], and tends to precipitate at high angle grain boundaries [25] (Figure 5a and 5b). Since the Mg contain in solid solution decreases, a decrease in lattice parameters of α_{Al} is expected as well [22].

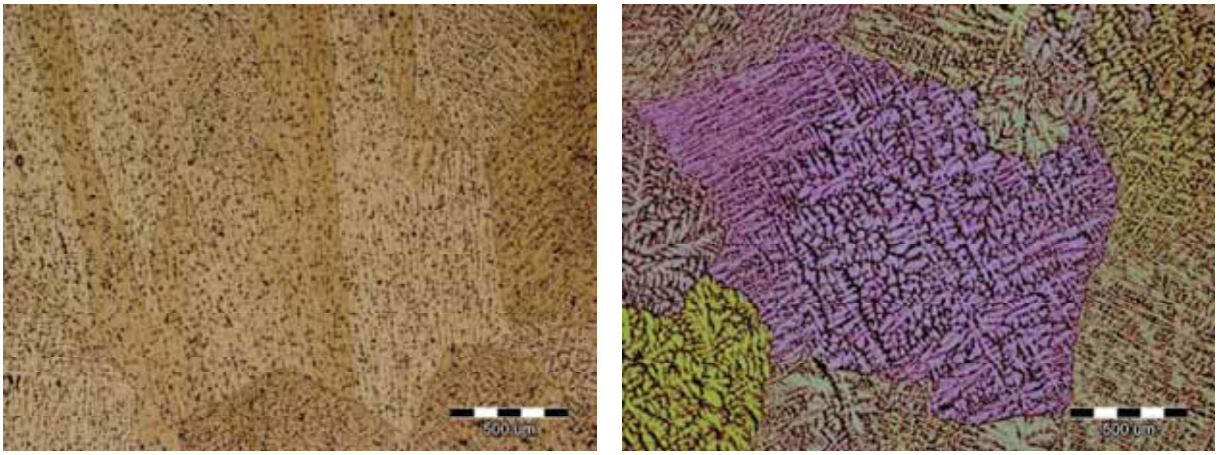

a) b)

Figure 5. Micrograph showing phase precipitations (predicted T phase) on the grain boundaries: a) between columnar and equiaxed zone, magnification 50X
b) in equiaxed zone, magnification 50X

Figure 5a and 5b shows regular spherical precipitates at the grain boundaries located between columnar and equiaxed zone. The quantitative line analysis is given in Figure 6.

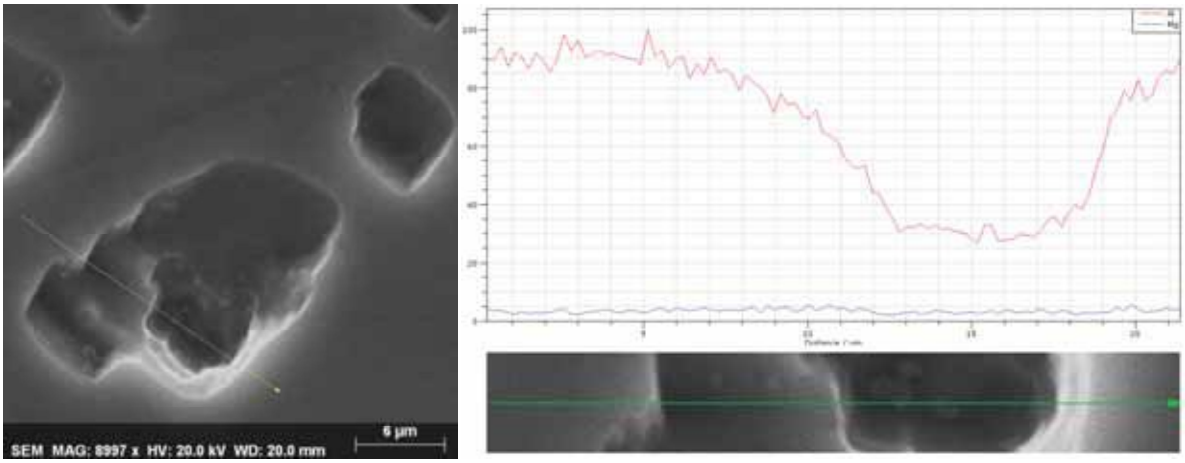

Figure 6. Quantitative microstructural analysis

However, results of line analysis, given in Figure 6, indicate no significant change in the Mg content between solid solution and phase precipitated at grain boundaries. Although, the α_{Al} becomes enriched in Mg, the following interaction with δ' will result in precipitation of T phase. Consequently, the parameters of α_{Al} lattice stay increased until eutectic reaction ($\alpha_{Al}'' \rightarrow \alpha_{Al}''' + Al_3Mg_2$) causes significant precipitation of Mg from the bulk α_{Al}''. Since Al_3Mg_2,

also known as Al_8Mg_5 [14] is the last solidifying phase, it will precipitate at the grain boundaries. The precipitates located at the grain boundaries are given in Figure 7a and 7b.

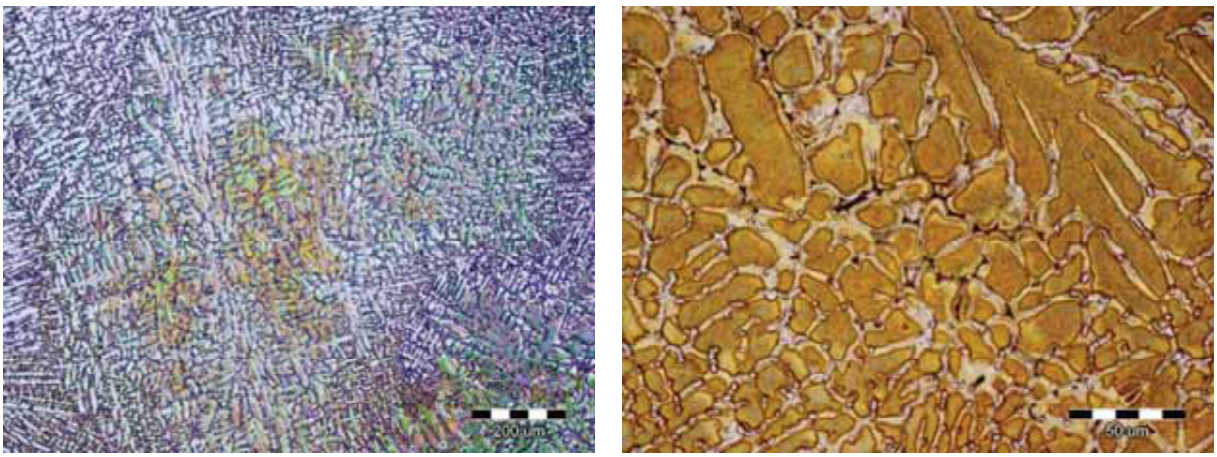

a) b)

Figure 7. Micrograph showing precipitations in interdendritic spaces of:
a) Fully formed dendrites at magnification 100X
b) Last solidifying area at magnification 200X

The areas between fragmented and fully formed dendrites represent the potential locations for precipitation of δ' (Figure 7a). Grain boundaries at the last solidifying areas are potential areas for Al_3Mg_2 precipitation, as shown in Figure 7b. The SEI and following mapping analysis is given if Figure 8a and 8b.

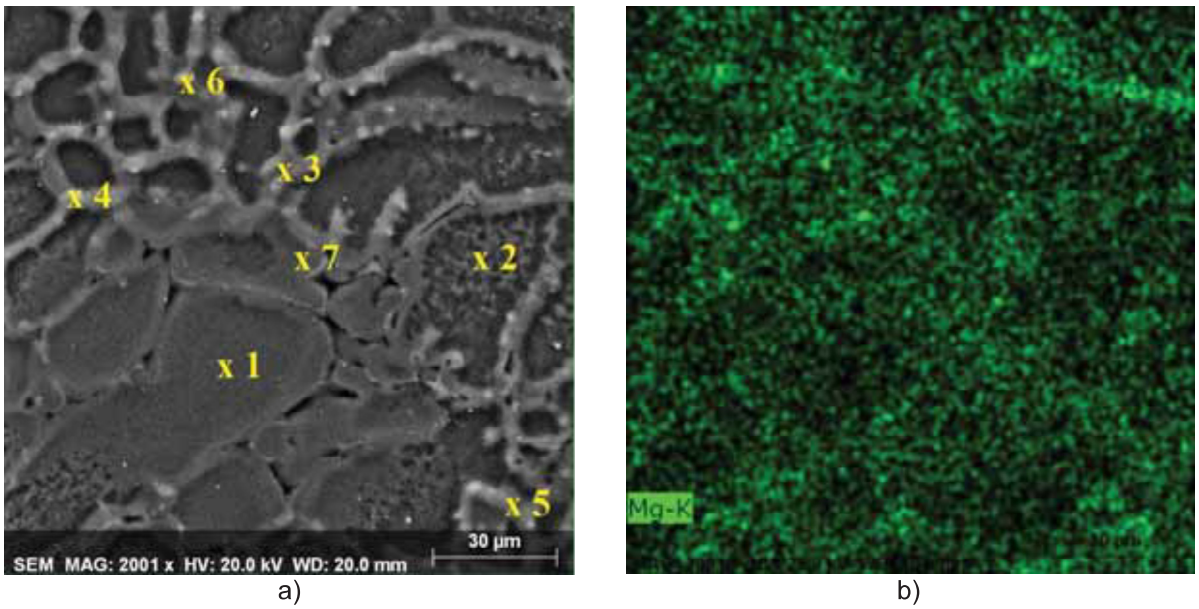

a) b)

Figure 8. SEI of:
a) Al - 2.5wt.%Mg – 0.7wt.%Li alloy with marked EDS analysis position
b) Mapping analysis of Mg content

Figure 8a shows SEI of densely distributed phases in both fragmented and fully developed dendrite areas, respectively. Since the results of mapping analysis have shown significant variations in colour intensity concerning Mg contains (Figure 8b), additional EDS quantitative microstructural analysis was done. The locations of EDS analysis are given in Figure 8a followed by chemical composition in Table 5.

Table 5. Results of EDS quantitative microstructural analysis

Location	Al, wt.%	Mg,wt.%
1	75.89	1.87
2	75.46	1.96
3	65.65	4.32
4	69.47	4.52
5	76.65	3.45
6	92.77	7.23
7	96.06	3.94

While the measurements taken at the location 1 and 2 confirm the existence of residual Mg in bulk α_{Al}, difference between measurements 3, 4, 5, 6 and 7 indicate the occurrence of different phases as well. Since EDS did not possess a possibility of light elements identification, prediction of present phases has been calculated from Al:Mg ratio. Comparison of Al:Mg ratio indicates presence of characteristic T phase.

Since the strengthening in Al-Li-Mg alloys is mainly done by metastable δ' precipitation, mechanical properties in as cast condition should be considered. Ultimately, in the as cast condition, Al_3Mg_2 and Al_2LiMg are the only identified secondary phases in α_{Al} matrix. Ternary T phase causes material softening because of Li deployment from δ' phase [25]. Since the Al_3Mg_2 precipitates as an irregular coarse particle at the grain boundaries, it cannot contribute to the strengthening effect [26]. However, since the stoichiometry of Al_3Mg_2 changes pending on Mg segregation and cooling rate, the amount of Mg left to increase the lattice parameters of α_{Al} lattice changes as well, consequently influencing strengthening potential of the alloy.

CONCLUSIONS

Correlation of predicted solidification sequence with microstructural analysis reveals identification of present constituents and theirs behaviour.

- Alloying with Mg and Li enable a significant decrease of casting density (ρ=2.489 g/cm^3) when compared to any commercial one.
- Lack of significant deviations in density between characteristic casting sections indicates no loss of Li during solidification neither by oxidation nor flotation processes.
- Mg addition decreases Li solubility in α_{Al} forcing the precipitation of metastable δ' phase, despite of low Li contents. Low Li/Mg ratio forces metastable δ' phase to decompose producing ternary T phase. During this peritectic reaction Li is first to deplete while the Mg contents in bulk α_{Al} stays unchanged.

- As the concentration of Mg increases in the bulk α_{Al}, the final eutectic reaction resulted in evolution of secondary eutectic Al_3Mg_2 phase.

So, even though, significant density reduction can be obtained by lower addition of Li – 0,7 wt.% and Mg – 2,5wt.%. Microstructure development and constituent's features are expected to have a significant influence on mechanical properties development.

REFERENCES

[1] N. Prasad, A. Eswara, A. Gokhale, R. J. H. Wanhill, Aluminium–lithium alloys, Aerospace Materials and Material Technologies Butterworth-Heinemann, Oxford, 2013.

[2] J. R. Santos, C. Mário, Machining of aluminum alloys: a review, The International Journal of Advanced Manufacturing Technology, 89(2016)9, pp. 3067-3080.

[3] R. Rajan, P. Kah, B. Mvola, J. Martikainen, Trends in Aluminium alloys development and their joining methods, Reviews on Advanced Materials Science, 44(2016)4, pp. 383-397.

[4] H. Buhl, Advanced aerospace materials, Springer Science & Business Media, Köln, 2012.

[5] M. Peters, C. Leyens, Aerospace and Space Materials, Material Science and Engineering, 3(2016)1, pp. 1-11.

[6] A. Akhtar, E. W. Akthar, S. J. Wu, Melting and casting of lithium containing aluminium alloys, International Jurnal of Cast Materials Research, 28(2015)1, pp. 1-8.

[7] C. Huang, A. J. Ardell, Determining the effect of microstructure and heat treatment on the mechanical strengthening behavior o fan aluminum alloy containing lithium precipitation hardened with the δ' Al3Li intermetallic phase, Journal of Materials Engineering and Performance, 9(2000)4, pp. 428-440.

[8] J. W. Martin, Aluminium-Lithium alloys, Ann. Rev. Mater. Sci, 18(1988)1, pp. 101-119

[9] C. J. Peel, B. Evans, R. Grimes, W. S. Miller, 9th Eur. Rotorcraft Forum, September 13-15, 1983, Stresa, Italy.

[10] K. K. Sankaran, N. J. Grant, The structure and properties of splat-quenched aluminium alloy 2024 containing lithium additions, Materials Science and Engineering, 44(1980)2, pp. 213-227.

[11] K. T. V. Rao, R. O. Ritchie, Fatigue of aluminium lithium alloys, International Materials Reviews 37(1992)4, pp. 153-185.

[12] J. Augustyn-Pieniążek, H. Adrian, S. Rzadkosz, M. Choroszyński, Structure and Mechanical Properties of Al-Li Alloys as Cast, Archives of Foundry Engineering, 13(2013)2, pp. 5-10.

[13] W. F. Hosford, Physical Metallurgy, CRC Press, New York, 2010.

[14] N. A. Belov, D. G. Eskin, A. A. Aksenov, Multicomponent phase diagrams: applications for commercial aluminum alloys Elsevier, 2006.

[15] R. K. Gupta, N. Nayan, G. Nagasireesha, S. C. Sharma, Development and characterization of Al-Li alloys, Materials Science and Engineering - Structural Materials Properties Microstructure and Processing, 420(2006)2, pp. 228-234.

[16] N. E. Prasad, S. V. Kamat, K.S. Prasad, G. Malakondaiah, V.V. Kutumbarao, Inplane anisotropy in the fracture-toughness of an Al-Li 8090-alloy plate, Engineering Fracture Mechanics, 46(1993)2, pp. 209-223.

[17] R. J. Rioja, Fabrication methods to manufacture isotropic Al-Li alloys and products for space and aerospace applications, Materials Science and Engineering A - Structural Materials Properties Microstructure and Processing, 257(1998)1, pp. 100-107.
[18] R. J. Rioja, J. Liu, The Evolution of Al-Li Base Products for Aerospace and Space Applications, Metallurgical and Materials Transactions A -Physical Metallurgy and Materials Science, 43(2012)9, pp. 3325-3337.
[19] M. Trinca, A. Avalino, H. Garmestani, J. Foyos, E. W. Lee, O. S. Es-Said, Effect of rolling orientation on the mechanical properties and crystallographic texture of 2195 aluminum-lithium alloy, 331(2000)1, pp. 849-854.
[20] N. E. Prasad, A. A. Gokhale, P. R. Rao, Mechanical behavior of aluminium-lithium alloys Sadhana, 28(2003)1, pp. 209-246.
[21] I. N. Fridlyander, N. I. Kolobnev, A. L. Berezina, K. V. Chuistov, The effect of scandium on decomposition kinetics in aluminium-lithium alloys, Aluminium-Lithium, 1-2(1992)1, pp. 107-112.
[22] S. Betsofen, M. Chizhikov, Quantitative Phase Analysis of Al-Mg-Li and Al-Cu-Li Alloys, Aluminium Alloys, 794(2014)1, pp. 915-920.
[23] S. Betsofen, V. Ya, V. Antipov, M.I. Knyazev, Al–Cu–Li and Al–Mg–Li alloys: Phase composition, texture, and anisotropy of mechanical properties (Review), Russian Metallurgy (Metally), 4(2016), pp. 326-341.
[24] A. Deschamps, C. Sigli, T. Mourey, F. de Geuser, W. Lefebvre, B. Davo, Experimental and modelling assessment of precipitation kinetics in an Al-Li-Mg alloy, Acta Materialia 60(2012)5, pp. 1917-1928.
[25] A. Mogucheva, R. Kaibyshev, Microstructure and Mechanical Properties of an Al-Li-Mg-Sc-Zr Alloy Subjected to ECAP, Metals, 6(2016)11, pp. 254.
[26] Z. Z. Brodarac, F. Unkic, J. Medved, P. Mrvar, Determination of solidification sequence of the AlMg9 alloy, Kovove Materialy-Metallic Materials, 50(2012)1, pp. 59-67.

Acknowledgements

This investigation has been performed in the frame of Financial support of investigation of University of Zagreb (TP167 “Design and characterization of innovative engineering alloys”) and collaboration between University of Zagreb Faculty of Metallurgy and University of Ljubljana Faculty of Natural Sciences and Engineering.